

Projected random forests and conformal prediction of circular data

Paulo C. Marques F.^{a,*}, Rinaldo Artes^a, Helton Graziadei^b

^aInspere Institute of Education and Research, Rua Quatá, 300, São Paulo, 04546-042, SP, Brazil

^bSchool of Applied Mathematics, Getulio Vargas Foundation, Praia de Botafogo, 190, Rio de Janeiro, 22250-900, RJ, Brazil

Abstract

We apply split conformal prediction techniques to regression problems with circular responses by introducing a suitable conformity score, leading to prediction sets with adaptive arc length and finite-sample coverage guarantees for any circular predictive model under exchangeable data. Leveraging the high performance of existing predictive models designed for linear responses, we analyze a general projection procedure that converts any linear response regression model into one suitable for circular responses. When random forests serve as basis models in this projection procedure, we harness the out-of-bag dynamics to eliminate the necessity for a separate calibration sample in the construction of prediction sets. For synthetic and real datasets the resulting projected random forests model produces more efficient out-of-bag conformal prediction sets, with shorter median arc length, when compared to the split conformal prediction sets generated by two existing alternative models.

Keywords: Circular Regression, Prediction Sets, Split Conformal Prediction, Projected Random Forests, Out-of-bag Conformal Prediction.

1. Introduction

Circular variables are used to represent attributes in a variety of domains, such as occurrence time of events [1, 2], orientation of phenomena in biological [3, 4], meteorological [5], ecological [6, 7, 8] and geological [9] problems, and measures of psychological traits based on the interpersonal circumplex [10]. The shared characteristic of these circular attributes is that they can be represented as angles, and specialized statistical concepts and methods [11, 12] are needed to account for the fact that, for instance, the radian values of two angles represent the same orientation in the plane if they differ by an integer multiple of 2π , manifesting the inherent periodicity of circular measurements.

In this study, we use conformal prediction techniques [13] to quantify the confidence in the forecasts made by general predictive models with circular response. We also examine a general projection procedure that transforms any predictive model originally designed for linear response variables into one suitable for circular responses. When applied to random forests [14], this projection procedure allows us to explore the out-of-bag conformalization technique introduced in [15], which eliminates the need for a separate calibration sample.

In Section 2, we show how split conformal prediction [16, 17] is implemented in our setting, proposing a circular conformity score that produces model-free prediction sets with finite-sample coverage guarantees for exchangeable data. The general projection procedure used to build circular predictive models

from existing methods with linear response is discussed in Section 3 and applied to random forests. The resulting projected random forests model is conformalized in a no-data-splitting manner, exploiting the availability of out-of-bag predictions for each training sample unit. We provide heuristics for the approximate validity of this out-of-bag conformal prediction procedure in the Appendix. In Section 4, we compare the out-of-bag conformal prediction sets produced by the projected random forests model to the split conformal prediction sets generated by two alternatives: the parametric projected normal linear regression model [18] and the semi-parametric circular forest [5]. For both synthetic and real datasets, the projected random forests model produces more efficient prediction sets, with shorter median arc length, for a batch of test predictions. We present final remarks in Section 5, giving pointers to our open source R [19] code and the data needed to reproduce all the discussed examples.

2. Conformity score for circular predictions

Consider a regression setting in which the data is randomly split into training and calibration samples, defining the data sequence

$$\underbrace{(X'_1, Y'_1), \dots, (X'_m, Y'_m)}_{\text{training}}, \underbrace{(X_1, Y_1), \dots, (X_n, Y_n)}_{\text{calibration}}, \underbrace{(X_{n+1}, Y_{n+1}), \dots}_{\text{future}}$$

We model the random pairs in this data sequence as being exchangeable. Each X'_i and X_i is a d -dimensional vector of explanatory variables and the response variables $Y'_i, Y_i \in [0, 2\pi)$ are angular measurements expressed in radians. The absolute difference between two given angles $\theta, \phi \in [0, 2\pi)$ is measured

*Corresponding author

Email addresses: PauloCMF1@insper.edu.br (Paulo C. Marques F.), RinaldoA@insper.edu.br (Rinaldo Artes), helton.carvalho@fgv.br (Helton Graziadei)

through the angular distance

$$\begin{aligned} d(\theta, \phi) &= \min\{|\theta - \phi|, 2\pi - |\theta - \phi|\} \\ &= \pi - |\pi - |\theta - \phi|| \in [0, \pi], \end{aligned}$$

which gives the length of the shortest arc between θ and ϕ in the unit circle.

From the information in the training sample $\{(X'_i, Y'_i)\}_{i=1}^m$, we build a first predictive model $\hat{\mu} : \mathbb{R}^d \rightarrow [0, 2\pi)$. Defining the circular training residuals $\Delta'_i = \pi - |\pi - |Y'_i - \hat{\mu}(X'_i)||$, a second variability model $\hat{\sigma} : \mathbb{R}^d \rightarrow (0, \pi]$ is constructed from the information in $\{(X'_i, \Delta'_i)\}_{i=1}^m$. We define the conformity scores for calibration and future sample units by

$$R_i = \frac{\pi - |\pi - |Y_i - \hat{\mu}(X_i)||}{\hat{\sigma}(X_i)}, \quad \text{for } i \geq 1.$$

Informally, the calibration sample conformity scores assess the out-of-sample predictive capacity of the model $\hat{\mu}$, and the distributional symmetry implied by the data exchangeability assumption transfers this assessment to the future observables, for which we become able to construct prediction sets with coverage guarantees without additional assumptions. The presence of the variability model $\hat{\sigma}$ in the conformity score denominator yields prediction sets with variable arc length for a batch of future observables, making the conformalization procedure more adaptable to the values of the explanatory variables [16, 17].

Briefly described, the classical split conformal prediction argument [16] proceeds as follows. Together, the data exchangeability assumption and the definition of the conformity score R_i imply that the vector of conformity scores $(R_1, \dots, R_n, R_{n+1})$ is exchangeable. Using the standard order statistics notation and considering that we may have ties among the conformity scores, it follows that at least k of the R_i 's are less than or equal to $R_{(k)}$, for $i, k = 1, \dots, n+1$; a fact that can be expressed in terms of indicator functions as $\sum_{i=1}^{n+1} I_{\{R_i \leq R_{(k)}\}} \geq k$, for $k = 1, \dots, n+1$. Taking expectations and noting that, by exchangeability, the probability $P(R_i \leq R_{(k)})$ is the same for every $i, k = 1, \dots, n, n+1$, it follows that

$$P(R_{n+1} \leq R_{(k)}) \geq \frac{k}{n+1}, \quad (1)$$

for $k = 1, \dots, n$. Let $\lceil t \rceil = \min\{k \in \mathbb{Z} : t \leq k\}$ denote the ceiling of $t \in \mathbb{R}$. For a nominal miscoverage level $0 < \alpha < 1$, such that $\lceil (1 - \alpha)(n+1) \rceil \leq n$, if we choose $k = \lceil (1 - \alpha)(n+1) \rceil$ in (1), and define $\hat{r} = R_{\lceil (1 - \alpha)(n+1) \rceil}$, we establish the lower bound $P(R_{n+1} \leq \hat{r}) \geq 1 - \alpha$. Additionally, if we have no ties among the conformity scores almost surely, adjusting the former argument to account for the fact that now exactly k of the R_i 's are less than or equal to $R_{(k)}$, and considering that $\lceil t \rceil < t + 1$, we get the upper bound $P(R_{n+1} \leq \hat{r}) < 1 - \alpha + 1/(n+1)$, firstly noted in [17].

In the no-ties case, it follows from the conformity score definition that

$$1 - \alpha \leq P\left(\bigcup_{\ell \in \mathbb{Z}} \{Y_{n+1} + 2\ell\pi \in C_n^{(\alpha)}(X_{n+1})\}\right) < 1 - \alpha + \frac{1}{n+1}, \quad (2)$$

in which, for $x \in \mathbb{R}^d$, the conformal prediction set is defined as

$$C_n^{(\alpha)}(x) = \{y \in [-\pi, 3\pi] : \hat{\mu}(x) - \hat{r} \cdot \hat{\sigma}(x) \leq y \leq \hat{\mu}(x) + \hat{r} \cdot \hat{\sigma}(x)\},$$

if $\hat{r} \cdot \hat{\sigma}(x) < \pi$, and $C_n^{(\alpha)}(x) = [0, 2\pi)$, otherwise. Of course, any periodic translation

$$C_n^{(\alpha)}(x) + 2\ell\pi = \{y + 2\ell\pi : y \in C_n^{(\alpha)}(x)\}, \quad \text{for } \ell \in \mathbb{Z},$$

gives a valid representation of the conformal prediction set satisfying the coverage property (2), and it is a matter of convention to report the conformal prediction set as a subset of $[-\pi, 3\pi]$.

3. Projected random forests

The widespread availability of open source software stacks implementing modern high-performance machine learning models designed for regression problems with linear response variables motivates the development of a general projection procedure enabling these models to serve as a basis for constructing predictive models suitable for problems with circular response, ultimately requiring no substantial additional software development. When the basis model is a random forest [14], this projection procedure leads naturally to an adaptation of the conformalization technique introduced in [15], which leverages the random forest out-of-bag dynamics to eliminate the need for a separate calibration sample. The resulting projected random forests model and its out-of-bag conformalization benefit from the availability of a larger training sample, resulting in a more efficient confidence assessment of the predictions made by the model.

Define $\mathbf{atan} : ([-1, 1] \times [-1, 1]) \setminus \{0, 0\} \rightarrow [0, 2\pi)$, by

$$\mathbf{atan}(c, s) = \begin{cases} \arctan(s/c) & \text{if } c > 0 \text{ and } s > 0; \\ \arctan(s/c) + \pi & \text{if } c < 0; \\ \arctan(s/c) + 2\pi & \text{if } c > 0 \text{ and } s < 0; \\ \pi/2 & \text{if } c = 0 \text{ and } s > 0; \\ 3\pi/2 & \text{if } c = 0 \text{ and } s < 0. \end{cases}$$

The general projection procedure works as follows. Two predictive models with linear response, $\hat{\mu}_c : \mathbb{R}^d \rightarrow [-1, 1]$ and $\hat{\mu}_s : \mathbb{R}^d \rightarrow [-1, 1]$, are built from the training samples

$$\{(X'_i, \cos(Y'_i))\}_{i=1}^m \quad \text{and} \quad \{(X'_i, \sin(Y'_i))\}_{i=1}^m,$$

respectively. The projected predictive model $\hat{\mu} : \mathbb{R}^d \rightarrow [0, 2\pi)$ is defined by $\hat{\mu}(X_i) = \mathbf{atan}(\hat{\mu}_c(X_i), \hat{\mu}_s(X_i))$, for $i \geq 1$.

From a conformal prediction standpoint, this projection procedure is particularly fruitful when random forests are used as basis models, due to the out-of-bag dynamics inherent to the random forest training process. The resulting projected random forests model and the construction of the corresponding out-of-bag conformal prediction sets are formally described in Algorithm 1. Throughout the algorithm, a resetting of the random seed is made to synchronize the bootstrap samples used in the four underlying random forests.

The out-of-bag conformal prediction sets produced by Algorithm 1 do not grant the same formal coverage guarantee (2) of split conformal prediction sets. Nevertheless, the experiments in Section 4 show that the empirical coverage of a batch

Algorithm 1 Out-of-bag conformal prediction using projected random forests

Input: Dataset $\{(x_i, y_i)\}_{i=1}^n$, with $x_i \in \mathbb{R}^d$ and $y_i \in [0, 2\pi)$, number B of trees used to train each random forest, random seed $\tau \in \mathbb{N}$, future vector of predictors $x_{n+1} \in \mathbb{R}^d$, and nominal miscoverage level $0 < \alpha < 1$.

Output: Prediction set.

```
1: Set the random seed to  $\tau$ 
2: Train random forest  $\{\hat{\mu}_c^{(j)}\}_{j=1}^B$  from  $\{(x_i, \cos(y_i))\}_{i=1}^n$ 
3: Reset the random seed to  $\tau$ 
4: Train random forest  $\{\hat{\mu}_s^{(j)}\}_{j=1}^B$  from  $\{(x_i, \sin(y_i))\}_{i=1}^n$ 
5: for  $i = 1$  to  $n$  do
6:    $O_i \leftarrow \{j : i\text{-th sample unit} \notin j\text{-th bootstrap sample}\}$ 
7:    $\delta_i \leftarrow \pi - \left| \pi - \left| y_i - \frac{1}{|O_i|} \sum_{j \in O_i} \text{atan}(\hat{\mu}_c^{(j)}(x_i), \hat{\mu}_s^{(j)}(x_i)) \right| \right|$ 
8:   Reset the random seed to  $\tau$ 
9:   Train random forest  $\{\hat{\sigma}_c^{(j)}\}_{j=1}^B$  from  $\{(x_i, \cos(\delta_i))\}_{i=1}^n$ 
10:  Reset the random seed to  $\tau$ 
11:  Train random forest  $\{\hat{\sigma}_s^{(j)}\}_{j=1}^B$  from  $\{(x_i, \sin(\delta_i))\}_{i=1}^n$ 
12:  for  $i = 1$  to  $n$  do
13:     $r_i \leftarrow \delta_i / \frac{1}{|O_i|} \sum_{j \in O_i} \text{atan}(\hat{\sigma}_c^{(j)}(x_i), \hat{\sigma}_s^{(j)}(x_i))$ 
14:     $\hat{y}_{n+1} \leftarrow \frac{1}{B} \sum_{j=1}^B \text{atan}(\hat{\mu}_c^{(j)}(x_{n+1}), \hat{\mu}_s^{(j)}(x_{n+1}))$ 
15:     $\epsilon \leftarrow r_{(\lceil (1-\alpha)(n+1) \rceil)} \times \frac{1}{B} \sum_{j=1}^B \text{atan}(\hat{\sigma}_c^{(j)}(x_{n+1}), \hat{\sigma}_s^{(j)}(x_{n+1}))$ 
16:    if  $\epsilon < \pi$  then
17:      return  $[\hat{y}_{n+1} - \epsilon, \hat{y}_{n+1} + \epsilon]$ 
18:    else
19:      return  $[0, 2\pi)$ 
```

of prediction sets generated by Algorithm 1 approximates the specified nominal level. In the Appendix, we present a heuristic argument to account for the approximate coverage property of general out-of-bag conformal prediction sets.

4. Experiments with synthetic and real data

In this section, we compare the split conformal prediction sets produced by the projected normal linear model and the circular forest (described in Sections 4.1 and 4.2, respectively) to the out-of-bag conformal prediction sets generated by the projected random forests model. The synthetic data generating process in Section 4.3 and the description of the circular forest in Section 4.2 rely on the von Mises distribution. A circular variable $Y \in [0, 2\pi)$ following a von Mises distribution with circular mean θ and concentration parameter $\kappa > 0$ has probability density function given by

$$f_Y(y) = \frac{\exp(\kappa \cos(y - \theta))}{2\pi I_0(\kappa)} \mathbb{I}_{[0, 2\pi)}(y),$$

in which I_0 is the modified Bessel function of the first kind of order 0.

4.1. Projected normal linear model

The projected normal linear model [18] introduces a set of real parameters and defines the response variable as the angle

generated by a unit vector. This unit vector is constructed by normalization of a vector following a bivariate normal distribution, with mean vector components defined by linear combinations involving the model parameters and the explanatory variables, and with an identity covariance matrix. The model parameters are estimated by maximum likelihood. See [18] for the technical details.

4.2. Circular forest

The circular forest model [5] is a bagging [20] of circular trees. Each circular tree is built by a recursive partitioning process involving the von Mises distribution. The process begins by fitting a von Mises distribution to the responses of the full training sample and generating a scoring matrix that measures how well the von Mises distribution fits each training sample unit. This scoring matrix is then tested for dependencies with each explanatory variable using permutation tests, thereby selecting one explanatory variable for the split. The best split point is found by maximizing a score discrepancy between the two resulting subgroups. This procedure is recursively applied to create further splits until a stopping criterion, such as minimal node size or lack of significant dependency, is met.

4.3. Synthetic data

The synthetic data generating process is the following. We simulate ten independent predictors x_1, \dots, x_{10} from a $U[-1, 1]$ distribution. The response variable $y \in [0, 2\pi)$ is drawn from a von Mises distribution with mean $2 \tan^{-1}(x_1 - 2x_2 + x_1x_2 - 2x_3^2) + \pi$ and concentration parameter $\kappa > 0$. The predictors x_4, \dots, x_{10} are introduced to create a degree of sparsity in the simulated dataset. We have training, calibration, and test samples with a size of 10,000. Figure 1 depicts the circular histogram for the response variable in the training sample, generated with concentration parameter $\kappa = 5$. When using Algorithm 1, we enlarge the training sample by adding to it the calibration sample, since the algorithm does not need a separate calibration sample to produce the prediction sets. The corresponding prediction intervals for fifty test sample units, produced by the three different methods, using a miscoverage level $\alpha = 0.1$, are shown in Figure 2. For the whole test sample, Table 1 gives the median and interquartile range of the arc lengths, and the empirical coverage for a batch of conformal prediction sets produced by the three different methods, for data generated with concentration parameters $\kappa \in \{1, 2, 5, 10\}$, using a nominal miscoverage level $\alpha = 0.1$. In all cases, Algorithm 1 produces more efficient prediction intervals, with smaller median arc length.

4.4. Wind direction data

We compiled hourly wind direction data from a meteorological station located in the Central-West region of Brazil, taking a sample through the period from January 1st, 2012, to July 30th, 2023. The raw data is publicly available at:

<https://tempo.inmet.gov.br/TabelaEstacoes/A001>

Table 1: Test sample median and interquartile range of the arc lengths, and empirical coverage for a batch of conformal prediction sets produced by the three different methods for synthetic data generated with different concentration parameters κ , using nominal miscoverage level $\alpha = 0.1$.

κ	Projected normal			Circular forest			Projected random forests		
	Median	IQR	Coverage	Median	IQR	Coverage	Median	IQR	Coverage
1	4.90	(0.74)	90.5%	4.84	(1.06)	90.6%	4.51	(0.71)	90.8%
2	4.05	(0.87)	90.2%	3.52	(0.85)	90.4%	2.96	(0.41)	90.1%
5	3.40	(1.20)	90.4%	2.09	(0.48)	89.9%	1.70	(0.25)	90.0%
10	3.21	(1.35)	89.6%	1.70	(0.62)	90.1%	1.24	(0.21)	89.9%

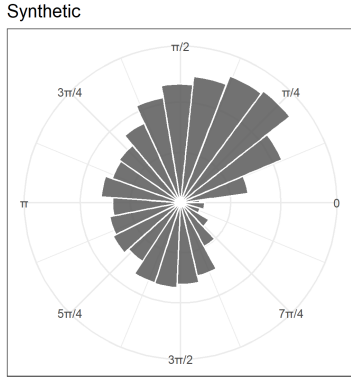


Figure 1: Circular histogram of the response variable in the synthetic dataset training sample, with concentration parameter $\kappa = 5$.

Table 2 gives a description of the available variables. We have training, calibration, and test sample units of sizes 10,000, 5,000, and 5,000, respectively. Figure 3 shows the circular histogram of the response variable in the training sample. Again, Algorithm 1 allows us to enlarge the training sample by adding to it the calibration sample. The prediction intervals for fifty test sample units, produced by the three different methods, using a miscoverage level $\alpha = 0.1$, are shown in Figure 4. For the whole test sample, Table 3 gives the median and interquartile range of the arc lengths, and the empirical coverage of the conformal prediction sets produced by the three different methods, using a nominal miscoverage level $\alpha = 0.1$. Again, Algorithm 1 outperforms the alternatives, producing prediction intervals with smaller median arc length.

Table 2: Variables in the wind direction dataset.

Variable	Unit
Wind direction	rad
Cosine of wind direction in the previous hour	dimensionless
Sine of wind direction in the previous hour	dimensionless
Total precipitation in the previous hour	mm
Atmospheric pressure in the previous hour	mB
Air temperature (dry bulb) in the previous hour	$^{\circ}\text{C}$
Dew point temperature in the previous hour	$^{\circ}\text{C}$
Relative humidity in the previous hour	%
Wind gust in the previous hour	m/s
Wind speed in the previous hour	m/s

Table 3: Median and interquartile range of the arc lengths, and empirical coverage for a batch of conformal prediction sets produced by the three different methods for the wind direction dataset, using nominal miscoverage level $\alpha = 0.1$.

	Median	IQR	Coverage
Projected normal	2.04	1.39	89.2%
Circular forest	2.23	3.07	90.2%
Projected random forests	1.90	1.87	89.5%

5. Concluding remarks

Open source software coded in R [19] and data for all the examples in the paper are available at:

<https://github.com/paulocmarquesf/circular>

We have two folders in this repository, named `synthetic` and `wind`, corresponding to the analyses of the respective datasets discussed in Section 4. Inside each folder, a suffix on a script name identifies the method used to produce the prediction intervals. Suffixes `projected_normal` and `circular_forest` refer to implementations of split conformal prediction, using the projected normal linear model and the circular forest, respectively. The suffix `projected_random_forests` refers to applications of Algorithm 1.

Acknowledgements

Paulo C. Marques F. receives support from FAPESP (Fundação de Amparo à Pesquisa do Estado de São Paulo) through project 2023/02538-0.

Appendix. Heuristics for out-of-bag conformal prediction

The experiments in Section 4 show that the out-of-bag conformal prediction sets exhibit an empirical coverage close to the specified nominal level. Since this calibration sample free conformalization procedure, introduced in [15], does not share the same formal coverage property (2) of split conformal prediction, this empirical performance motivates the search for an adequate theoretical basis. Although there is no complete theory for the coverage properties of out-of-bag conformal prediction sets, the heuristic argument presented below aims to convey some understanding of the theoretical underpinnings behind the

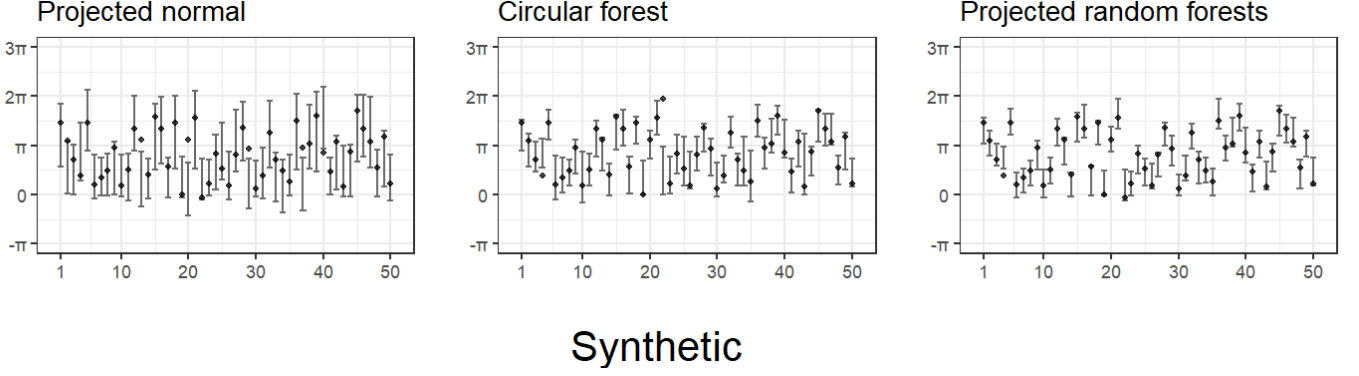


Figure 2: Prediction intervals for fifty test sample units in the synthetic dataset, with $\kappa = 5$, produced by the three different methods, using a miscoverage level $\alpha = 0.1$. The black dots are the observed circular responses.

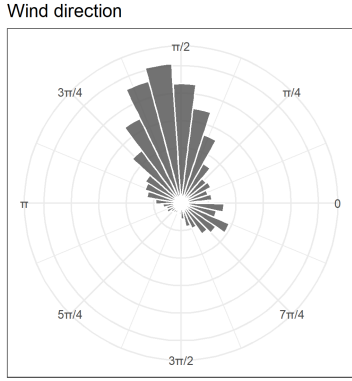


Figure 3: Circular histogram of the response variable in the wind direction dataset training sample

empirically observed behavior. To simplify the discussion and to emphasize the generality of the argument, we frame our exposition to the case of standard regression problems with linear response, using the simplest possible conformity score. The argument extends directly to more general settings.

The loss of the coverage property (2) when we move from split conformal prediction to the out-of-bag procedure is due to the fact that we no longer have the same predictive model being used to compute each of the underlying conformity scores. In fact, the use of out-of-bag predictions to compute the training sample conformity scores implies that each score is computed using a different predictive model: the subforest for which the training sample unit stayed out-of-bag during the bootstrap process. This modification breaks the original distributional symmetry making the conformity scores no longer exchangeable. Our strategy is to symmetrize the out-of-bag conformal prediction procedure making two practically prohibitive changes. First, we consider an idealized random forest built from an exhaustive bootstrap process which includes all possible bootstrap samples. Second, we add the future sample unit to the training sample. If we are able to move from this idealized scenario to an actual random forest, controlling the distribution of some specific differences, then we can show that the out-of-bag conformal prediction sets satisfy a coverage property with a lower

bound close to the one established for split conformal prediction in Section 2.

Suppose that the pairs $(X_1, Y_1), \dots, (X_n, Y_n), (X_{n+1}, Y_{n+1})$ are exchangeable, with $X_i \in \mathbb{R}^d$ and $Y_i \in \mathbb{R}$. Consider an exhaustive bootstrap of this extended training sample, which includes the pair (X_{n+1}, Y_{n+1}) , producing all possible $\tilde{B} = (n+1)^{n+1}$ samples with replacement of size $n+1$. Let $\tilde{O}_i \subset \{1, \dots, \tilde{B}\}$ be the indices of the bootstrap samples for which the i -th sample unit was not included (stayed “out-of-bag”), for $i = 1, \dots, n+1$. Note that $|\tilde{O}_i| = n^{n+1}$ and $|\tilde{O}_i|/\tilde{B} \rightarrow e^{-1} = 0.3678 \dots$. A regression tree is built from each bootstrap sample. Since Breiman [14] introduced a random selection of the available explanatory variables as candidates to decide each tree branch split, we set the random seed to an integer obtained by applying any symmetric hashing function to the bootstrap sample before training each regression tree, in order to maintain the symmetry of the whole procedure. This process results in the idealized random forest $\widetilde{\text{RF}} = \{\tilde{\mu}^{(j)}\}_{j=1}^{\tilde{B}}$.

Defining the idealized out-of-bag conformity scores

$$\tilde{R}_i = \left| Y_i - \frac{1}{|\tilde{O}_i|} \sum_{j \in \tilde{O}_i} \tilde{\mu}^{(j)}(X_i) \right|$$

for $i = 1, \dots, n+1$, if we specify a nominal miscoverage level $0 < \alpha < 1$, such that $\lceil (1-\alpha)(n+1) \rceil \leq n$, and define $\tilde{r} = \tilde{R}_{(\lceil (1-\alpha)(n+1) \rceil)}$, the data exchangeability assumption and the completely symmetric process used to define the idealized random forest $\widetilde{\text{RF}}$ yields the following result, by applying the same combinatorial reasoning used to prove property (2) in Section 2.

Lemma 1. *The random vector $(\tilde{R}_1, \dots, \tilde{R}_n, \tilde{R}_{n+1})$ is exchangeable and $P(\tilde{R}_{n+1} \leq \tilde{r}) \geq 1 - \alpha$.*

We now move to an actual random forest $\text{RF} = \{\hat{\mu}^{(j)}\}_{j=1}^B$, built from a usual bootstrap process involving a manageable number of B samples of size n obtained with replacement from the training sample $(X_1, Y_1), \dots, (X_n, Y_n)$, which no longer includes the future pair (X_{n+1}, Y_{n+1}) . Let $O_i \subset \{1, \dots, B\}$ be the indices of the bootstrap samples for which the i -th sample unit was not included, for $i = 1, \dots, n$. Define the out-of-bag train-

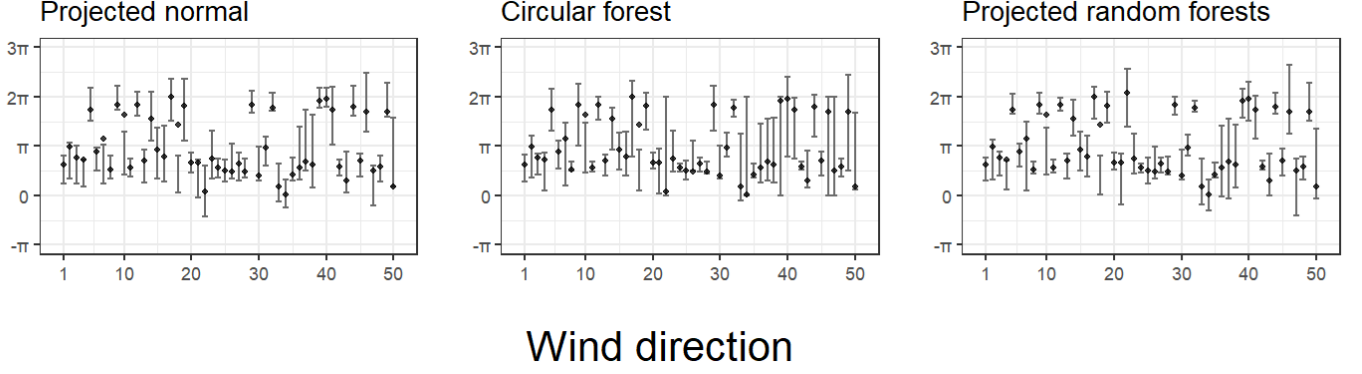


Figure 4: Prediction intervals for fifty test sample units in the wind direction dataset, produced by the three different methods, using a miscoverage level $\alpha = 0.1$. The black dots are the observed wind directions.

ing sample conformity scores

$$R_i = \left| Y_i - \frac{1}{|O_i|} \sum_{j \in O_i} \hat{\mu}^{(j)}(X_i) \right|,$$

for $i = 1, \dots, n$, and the conformity score for the future sample unit

$$R_{n+1} = \left| Y_{n+1} - \frac{1}{B} \sum_{j=1}^B \hat{\mu}^{(j)}(X_{n+1}) \right|.$$

Defining $\hat{r} = R_{(\lceil(1-\alpha)(n+1)\rceil)}$, the key idea is that if n and B are large enough, the stability of the random forest algorithm would allow us to move from the idealized random forest $\widehat{\mathbf{R}}F$ to the actual random forest RF, controlling the probability that R_{n+1} and \tilde{R}_{n+1} , as well as \hat{r} and \tilde{r} , differ too much. The following result formalizes this idea.

Theorem 1. *If for every $\epsilon > 0$ there exists a $\delta = \delta(\epsilon) > 0$, such that*

$$P\left(\max\{|R_{n+1} - \tilde{R}_{n+1}|, |\hat{r} - \tilde{r}|\} < \epsilon/2\right) \geq 1 - \delta,$$

then

$$P(R_{n+1} \leq \hat{r}) \geq 1 - \alpha - \delta - h(\epsilon),$$

in which $h(\epsilon) = P(\tilde{r} - \epsilon < \tilde{R}_{n+1} \leq \tilde{r})$. Furthermore, if the joint distribution of the idealized conformity scores is absolutely continuous, then $\lim_{\epsilon \downarrow 0} h(\epsilon) = 0$.

Proof. If $\max\{|R_{n+1} - \tilde{R}_{n+1}|, |\hat{r} - \tilde{r}|\} < \epsilon/2$ and $\tilde{R}_{n+1} \leq \tilde{r} - \epsilon$, then $R_{n+1} < \tilde{R}_{n+1} + \epsilon/2 \leq \tilde{r} - \epsilon/2 < \hat{r}$. Defining the event $B_\epsilon = \{\max\{|R_{n+1} - \tilde{R}_{n+1}|, |\hat{r} - \tilde{r}|\} < \epsilon/2\}$, and using Lemma 1, we have the first claim:

$$\begin{aligned} P(R_{n+1} \leq \hat{r}) &\geq P(\{R_{n+1} < \hat{r}\} \cap B_\epsilon) \\ &\geq P(\{\tilde{R}_{n+1} \leq \tilde{r} - \epsilon\} \cap B_\epsilon) \\ &= P(\tilde{R}_{n+1} \leq \tilde{r} - \epsilon) - P(\{\tilde{R}_{n+1} \leq \tilde{r} - \epsilon\} \cap B_\epsilon^c) \\ &\geq P(\tilde{R}_{n+1} \leq \tilde{r} - \epsilon) - P(B_\epsilon^c) \\ &\geq P(\tilde{R}_{n+1} \leq \tilde{r} - \epsilon) - \delta \\ &= P(\tilde{R}_{n+1} \leq \tilde{r}) - P(\tilde{r} - \epsilon < \tilde{R}_{n+1} \leq \tilde{r}) - \delta \\ &\geq 1 - \alpha - \delta - P(\tilde{r} - \epsilon < \tilde{R}_{n+1} \leq \tilde{r}). \end{aligned}$$

The second claim is immediate. \square

Recalling from the discussion in Section 2 that the lower bound on the coverage property (2) follows directly from the lower bound on the probability $P(R_{n+1} \leq \hat{r})$, we come to an intuition of why the empirical coverage of out-of-bag conformal prediction sets stays close to the specified nominal level in our experiments.

References

- [1] J. Gill, D. Hangartner, Circular data in political science and how to handle it, *Political Analysis* 18 (3) (2010) 316–336.
- [2] M. G. Leguia, R. G. Andrzejak, C. Rummel, J. M. Fan, E. A. Mirro, T. K. Tcheng, V. R. Rao, M. O. Baud, Seizure cycles in focal epilepsy, *JAMA Neurology* 78 (4) (2021) 454–463.
- [3] M. H. Ali, M. Ray, S. R. Jammalamadaka, S. Senthil, M. Srinivas, S. Pyne, Focused analysis of RNFL decay in glaucomatous eyes using circular statistics on high-resolution OCT data, *PLOS ONE* 18 (10) (2023) e0292915.
- [4] L. Landler, G. D. Ruxton, E. P. Malkemper, Circular data in biology: advice for effectively implementing statistical procedures, *Behavioral ecology and sociobiology* 72 (2018) 1–10.
- [5] M. N. Lang, L. Schlosser, T. Hothorn, G. J. Mayr, R. Stauffer, A. Zeileis, Circular regression trees and forests with an application to probabilistic wind direction forecasting, *Journal of the Royal Statistical Society Series C: Applied Statistics* 69 (5) (2020) 1357–1374.
- [6] B. S. Otieno, C. M. Anderson-Cook, Measures of preferred direction for environmental and ecological circular data, *Environmental and Ecological Statistics* 13 (2006) 311–324.
- [7] R. R. Fitak, S. Johnsen, Bringing the analysis of animal orientation data full circle: model-based approaches with maximum likelihood, *Journal of Experimental Biology* 220 (21) (2017) 3878–3882.
- [8] M. Ranalli, A. Maruotti, Model-based clustering for noisy longitudinal circular data, with application to animal movement, *Environmetrics* 31 (2) (2020) e2572.
- [9] R. Lark, D. Clifford, C. Waters, Modelling complex geological circular data with the projected normal distribution and mixtures of von mises distributions, *Solid Earth* 5 (2) (2014) 631–639.
- [10] J. Cremers, H. J. Pennings, T. Mainhard, I. Klugkist, Circular modelling of circumplex measurements for interpersonal behavior, *Assessment* 28 (2) (2021) 585–600.
- [11] K. V. Mardia, P. E. Jupp, K. Mardia, *Directional Statistics*, John Wiley & Sons, Inc., 1999.
- [12] A. Pewsey, E. García-Portugués, Recent advances in directional statistics, *Test* 30 (1) (2021) 1–58.
- [13] V. Vovk, A. Gammerman, G. Shafer, *Algorithmic learning in a random world*, Springer Science & Business Media, 2005.
- [14] L. Breiman, Random Forests, *Machine Learning* 45 (1) (2001) 5–32.

- [15] U. Johansson, H. Boström, T. Löfström, H. Linusson, Regression conformal prediction with random forests, *Machine learning* 97 (2014) 155–176.
- [16] H. Papadopoulos, K. Proedrou, V. Vovk, A. Gammerman, Inductive confidence machines for regression, in: T. Elomaa, H. Mannila, H. Toivonen (Eds.), *Machine Learning: ECML 2002*, Springer Berlin Heidelberg, Berlin, Heidelberg, 2002, pp. 345–356.
- [17] J. Lei, M. G’Sell, A. Rinaldo, R. J. Tibshirani, L. Wasserman, Distribution-free predictive inference for regression, *Journal of the American Statistical Association* 113 (523) (2018) 1094–1111.
- [18] B. Presnell, S. P. Morrison, R. C. Littell, Projected multivariate linear models for directional data, *Journal of the American Statistical Association* 93 (443) (1998) 1068–1077.
- [19] R Core Team, *R: a language and environment for statistical computing*, R Foundation for Statistical Computing, Vienna, Austria (2021).
URL <https://www.R-project.org/>
- [20] L. Breiman, Bagging predictors, *Machine Learning* 24 (2) (1996) 123–140.